2022 19th International Conference Electrical Engineering, Computing Science and Automatic Control (CCE)
Mexico City, Mexico. November 9-11, 2022.

Effect of thermal annealing on the photoluminescence properties of bilayer arrays of SiO_2 and TiO_2 nanospheres and its application as down conversion layers in c-Si solar cells

Carina Gutierrez
Optics
National Institute for Astrophysics Optics and Electronics, INAOE.
Puebla, Mexico.
carina.gutierrez@inaoep.mx

Mario Moreno
Electronics
National Institute for Astrophysics Optics and Electronics, INAOE.
Puebla, Mexico.
mmoreno@inaoep.mx

Ponciano Rodríguez
Optics
National Institute for Astrophysics Optics and Electronics, INAOE.
Puebla, Mexico.
ponciano@inaoep.mx

Alfredo Morales
Electronics
National Institute for Astrophysics Optics and Electronics, INAOE.
Puebla, Mexico.
alfredom@inaoep.mx

Víctor Aca
Electronics
National Institute for Astrophysics Optics and Electronics, INAOE.
Puebla, Mexico.
avictor@inaoep.mx

Leticia Tecuapetla
Electronics
National Institute for Astrophysics Optics and Electronics, INAOE.
Puebla, Mexico.
ltecuap@inaoep.mx

***Abstract*— Experimental results on the influence of the annealing temperature on the photoluminescence (PL) emission of silica and Titania arrays are presented. Bilayers of titania and silica nanoparticles (NPs) of 100 nm and 600 nm, respectively, were deposited on crystalline silicon (c-Si) substrates and exposed to an annealing process from 400°C to 1100°C in a controlled atmosphere. Our results show that PL intensity emissions can be switched controlling the annealing temperature for 30 minutes. Annealing parameters from bilayer NPs results are applied as absorber layers in c-Si solar cells to enhance their performance characteristic.**

Keywords—Photoluminescence, reflectance, Titania, Silica, nanoparticles, solar cells.

I. INTRODUCTION

Nature is the main protagonist of important phenomena that include inert materials and living organisms. Scientists through different mechanisms try to describe these phenomena with film interference, diffraction grating, scattering, and phonic crystal principles [1]. One way to achieve a mimic of these structures is with micro- or nano-structures allowing interaction with the wavelength. According to the phenomena corresponds to the structural design that describes the process. Some structures are based on plasmonic structures such as nanoholes, metal-insulator-metal, nanorods, nanopillars, nanowires, grating, or dielectric structures as nanospheres. An application of this kind of structures is the light trapping mechanism based on focusing, waveguiding, and scattering, as a leaf does through arrangements of dielectric spherical structures as some authors report [2], [3], [4], where the shape, size, and material can control the amount of incident light to be captured into itself. Therefore, these kinds of geometries have been studied for solar energy harnessing.

Conversely, photovoltaic (PV) systems have some issues to establish a reliable source of electrical power, for example, their low energy density. Conventional solar cells exhibit relatively low conversion efficiencies due to several issues, as reflection losses, lattice thermalization, recombination, parasitic resistances [5], but the most important is the fact that there is not any material capable to absorb the 100 percent of light (UV-Visible-IR). Therefore, one possible solution is the implementation of films or structures in the top of the solar cells in order to absorb more efficiently the solar spectrum. Which can be achievable with the Down conversion (DC) process, where a high-energy photon is converted into two or more photons with lower energy [5].

Early works related to DC for solar cell applications were focused on lanthanide ions due to their optical properties [5]. However, the silicon dioxide (Silica) and titanium dioxide (Titania) nanomaterials arrangements, studied as light trapping, are an option as down converters due to their photoluminescence (PL) properties. It is possible that, from their spherical NPs configuration and their material properties could guide the incident light into the NPs array and then maximize the scattering, improving a light absorption. The Titania nanoparticles (NPs) properties are two crystal phases, anatase and rutile, with a refractive index of 2.4 and 2.9, respectively, while their band gap is about 3.2 eV for the anatase phase and 3.05 eV for the rutile phase [6]. The Silica NPs have a refractive index of 1.47 and a reported band gap of 3.85 eV [7]. Analyzing different configurations has an important role for the reduction of reflection losses.

The optical properties of nanostructured semiconductors can be modified under thermal treatment to improve the efficiency of light sources for some optoelectronic devices. PL and the mechanism of light emission in thermal annealed thin films have been widely studied, for example, in the silicon excess in silicon-rich oxide (SRO) films and TiO_2-SiO_2 films [8], [9]. Performance of the dependence of the PL peak energy and its intensity enhancement as a function of the annealing time was studied in [10] and [11]. For example, PL intensity of Titania nanostructures studies under annealing time

978-1-6654-5508-4/22/$31.00 ©2022 IEEE

variation showed a PL enhanced at short times from 400 nm to 800 nm [8] at 1100°C. Also, studied films of SiO_2 exhibited a PL band in the 1.4-2.1 eV range after being exposed at 1100°C for 1, 3, and 5 hours [12]. These results were explained by the change in surface trap levels, which are induced by the presence of oxygen vacancies [13], [14].

We propose experimentally to study the Silica and Titania NPs photoluminescent enhancement by annealed treatment with variation in temperature. In this report, study the PL properties of nanoparticles array of silica and titania, with a diameter of 600 nm and 100 nm, respectively, and then we select the best temperature parameters to apply the films over conventional c-Si solar cells to enhance their performance characteristics.

II. Experimental

A. Materials

Silica (SiO_2) nanoparticles (NPs) with an average diameter of 600 nm at 5 wt% in water and Titania NPs in rutile phase and high purity with an average diameter of 100 nm at 20 wt% in water were purchased from NanoCym and US Research Nanomaterials, Inc., respectively. As substrates, we employed [100] crystalline silicon (c-Si) substrates. Standard c-Si solar cells (1×1 cm^2) were fabricated and proportionated by the microelectronics lab from INAOE.

B. Substrate preparation

c-Si substrates were prepared using two processes. The first process was the cleaning process which includes the c-Si solar cells: the substrates were immersed in an ultrasonic shower with Trichloroethylene (TCE) and then in acetone, 10 min for each solvent, washed three times in deionized water, and dried by centrifuge. The second process makes hydrophilic surfaces, the substrates were exposed to oxygen plasma at 300 W and 250 mTorr for 240 s.

C. Colloidal solution preparation

Silica and Titania NPs were received as a colloidal suspension in water. The NPs were dispersed in a ratio of 1:3 and 1:2, respectively, with a solution of the surfactant Triton X-10 and methanol at 1:400 by volume [15], [16]. The NPs suspensions were sonicated for 30 min to avoid agglomeration.

D. Nanospheres deposition

Two periodic silica and titania arrays were deposited on c-Si substrates of size 1×1 in. The first array is a Silica-Titania bilayer, the silica NPs form the bottom monolayer and titania NPs form the top monolayer. The NPs layer was deposited at a spin speed of 1500 rpm, and 4000 rpm, respectively, see Figure 1a). The second array is a Titania-Silica bilayer, the titania NPs form the bottom monolayer and silica NPs form the top layer, Figure 1b). The rpm is the same that another configuration. Every NPs layer was dried at 80°C for 10 minutes on a hotplate. The Titania-Silica NPs configuration was deposited on the top of the c-Si solar cell shown in Figure 2a). The NPs bilayer configuration does not cover all the Al contacts, see Figure 2b).

E. Thermal annealing of NPs bilayer array

The Silica-Titania and Titania-Silica samples were annealed at 400, 500, 600, 700, 800, 900, 1000, and 1100°C for 30 minutes in a tube furnace with a flat quartz holder, under a nitrogen atmosphere at atmospheric pressure to study the PL emission. The Titania-Silica configuration on c-Si solar cells was annealed at 400°C for 5, 10, 20, and 30 min, and 500°C for 10, 20, and 30 min.

F. Characterization equipment

The periodical NPs distribution was visualized by a Scanning Electron Microscope (SEM) Hitachi, model SU3500. Photoluminescence spectra were recorded at room temperature in the wavelength range of 370-1000 nm using a photomultiplier tube as a signal detector. The 3.54 eV (350 nm) emission line of a continuous light source xenon arc lamp was used for the excitation. The phase contrast was measured with the AFM equipment (Besoke Delta Phi). The Titania-Silica configuration on c-Si solar cells was measured with a Solar simulator AM1.5 with a power density of 100mW/cm^2.

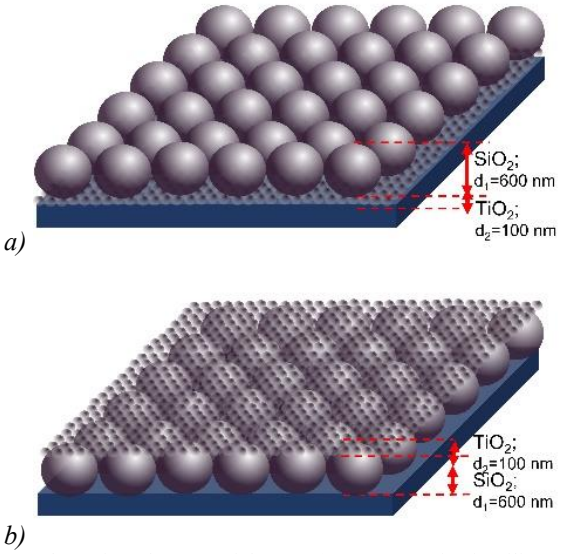

Figure 1. Schematics of nanoparticles (NPs) arrays: a) Titania-Silica NPs configuration and b) Silica-Titania NPs configuration.

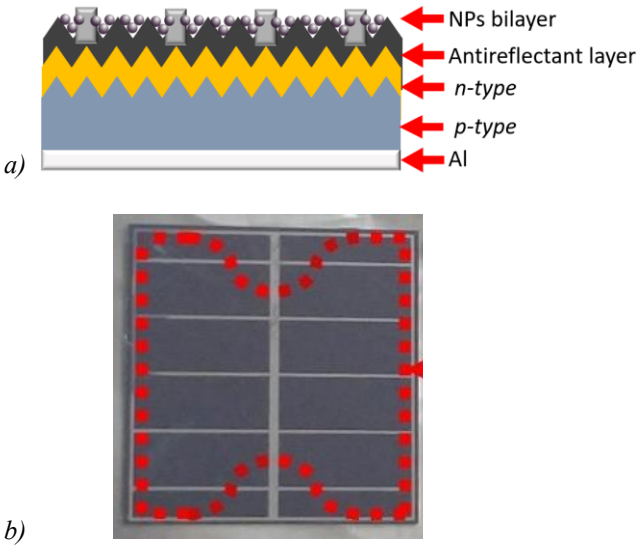

Figure 2. a) Basic structure of a c-Si solar cell and b) NPs deposited inside the red dashed line on the c-Si solar cell of 1×1 cm dimension.

III. Results and Discussion

A. Morphology

Figure 3 shows the images of nanoparticles (NPs) configurations obtained by Scanning Electron Microscopy. Figure 3 a) shows the Titania-Silica NPs configuration. The bottom layer of titania NPs appears to be a uniform NPs layer at a spin speed of 4000 rpm. Meanwhile, the top layer of Silica NPs is closely distributed at 1500 rpm. Figure 3 b) shows the Silica-Titania NPs configuration. The bottom monolayer of silica NPs shows holes between the dispersed NPs at 1500 rpm. There is observed that the top layer of titania NPs does not have a uniform distribution although they were distributed at 4000 rpm.

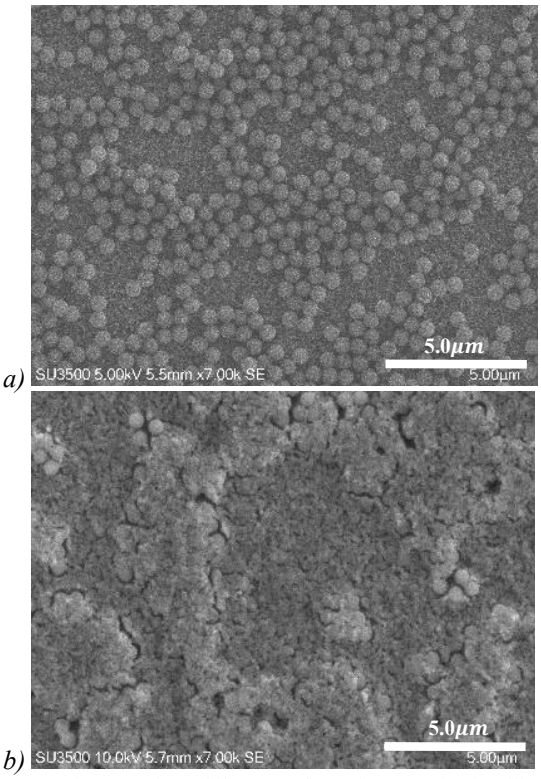

Figure 3. SEM images of NPs bilayer configurations: a) Titania-Silica NPs configuration: the bottom layer is made with titania NPs with 1:2 concentration deposited at 4000 rpm and the top NPs layer is made with silica NPs with a concentration of 1500 rpm, and b) is the Silica-Titania NPs configuration, it is made with the same parameters than another configuration.

To identify a morphology change, in Figure 4 is shown the phase contrast of the NPs monolayer before and after the thermal treatment. Figure 4a) illustrates the phase contrast of Titania NPs monolayer without thermal treatment, while Figure 4b) shows the same monolayer thermaly annealed at 1100 °C for 30 minutes. There is observed a smoothing between the NPs distribution after the annealing process. Similarly, Figure 4c) shows the Silica NPs monolayer without thermal treatment and Figure 4d) shows the same sample thermaly annealed at 1100 °C for 30 minutes. These images show that Silica NPs after thermal treatment are melting, then, there is a greater contact area between the NPs because their spherical shape is modified to ellipsoids. Therefore, is expected that NPs at high temperatures suffer a mechanical and structural restructuring. These results were corroborated with the roughness decrease; Titania NPs roughness (RMS) changes from 0.0296 μm to 0.281 μm, and Silica NPs changes from 0.0464 μm to 0.0425 μm, at 25 °C and 1100 °C, respectively.

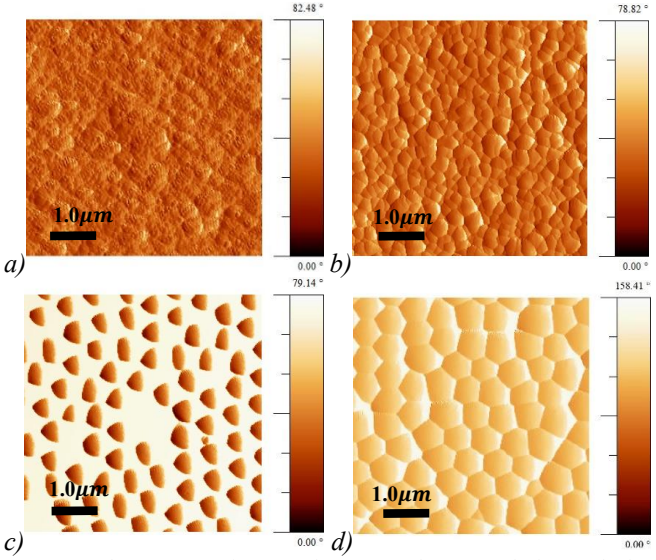

Figure 4. Phase contrast images of NPs monolayer NPs before and after annealing process: a) Titania NPs without thermal treatment, b) Titania NPs thermally annealed at 1100 °C for 30 minutes, c) Silica NPs before thermal treatment and d) Silica NPs thermally annealed at 1100 °C for 30 minutes.

Photoluminescence

Figure 5 shows the characteristic PL spectra of NPs bilayer configurations before the thermal treatments. The black line represents the PL emission of the Titania-Silica configuration, there is observed that the maximum emission achieves the 1800 a.u. in the wavelength of 400 nm that is associated with the silica PL emission [12], and there is a second emission with a lower amplitude of 500 a.u in the wavelength range of 750 and 850 nm that is associated with the characteristic titania PL emissions [8]. The red line shows the PL spectra of the Silica-Titania configuration. There is observed a unique maximum emission in the wavelength of 400 nm that corresponds to the silica NPs emission.

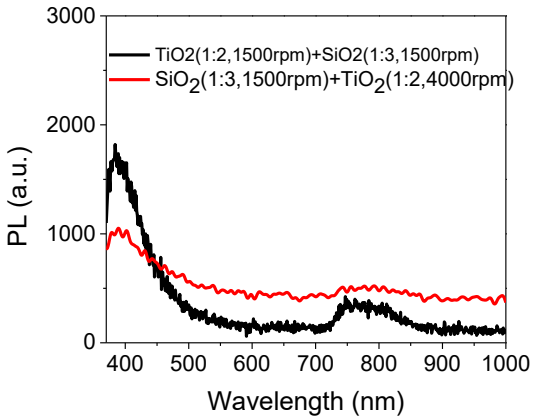

Figure 5. Photoluminescence of NPs bilayer configuration of a) Titania-Silica configuration and b) Silica-Titania configuration before thermal treatment.

Experimental results show that the NPs monolayer order contributes to the PL intensity emission. Is observed that the silica NPs monolayer on the top of the configuration increase

and sharp the two PL emissions at 400 nm and 800 nm, when the silica NPs monolayer is on the bottom the PL intensity is decreased by the existence of titania NPs.

Conversely, Figure 6 shows the PL spectra of the NPs bilayer configurations with thermal treatments from 400 to 1100°C with steeps of 100°C. Figure 6a) shows the PL spectra of Titania-Silica NPs configuration. There is observed two PL emissions at 400 nm and 800 nm. It is important to highlight a change in the PL intensity as the temperature increase. For a temperature of 400°C, the PL emission reaches the maximum emission of 10000 a.u. in 400 nm, almost 5 times higher than the non-annealed sample. Also, the second emission at 800 nm reaches a PL intensity of 2000 a.u. As the temperature is increased, the PL emission decreases gradually at 400 nm and is observed also that the PL intensity increases at 800 nm. The maximum PL emission reached in 800 nm is around 8000 a.u. for a temperature of 1000°C and it represents 27 times largest than samples without thermal treatment. Therefore, the maximum PL of Titania-Silica NPs configuration shows an intensity transition from 400 nm to 800 nm when an increment in temperature is applied.

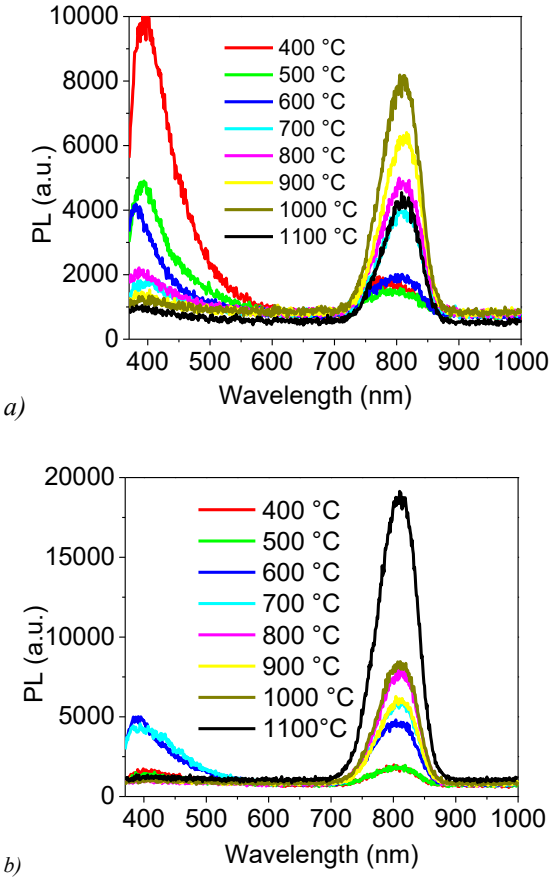

Figure 6. Photoluminescence of NPs bilayer configuration of a) Titania-Silica configuration and b) Silica-Titania configuration with thermal treatment from 400 to 1100°C for 30 minutes.

Figure 6b) shows the PL spectra of Silica-Titania NPs configuration, there is observed two PL emission peaks. The first peak is at 400 nm, where the maximum PL amplitude reached is around 2000 a.u for temperatures from 400 to 1100°C, this PL intensity is 2 times larger than the sample without thermal treatment. There is a second peak at 800 nm, the maximum amplitude reached is 20000 a.u. and it is 400 times larger than samples without thermal treatment. There is observed that the PL intensity for this configuration increase as temperature increases in the IR region.

From these results, when the NPs configurations are exited with an energy of 3.54 eV two emission are presented, one of them at 3.1 eV associated with silica NPs emission and the second one at 1.55 eV corresponding to titania NPs. The amplitude change is related with the annealing temperature applied, because, annealing temperatures higher than 500 °C shows a slight increase in the presence of titanium in the material and a slight absence of oxygen, which indicates that titanium has changed in their molecular structure, where oxygen vacancies are generated by desorption [17]. On the other hand the silica is affected by the size and structure of the nanocrystals that structuring the NPs [12].

Our experimental results show that NPs bilayer order modifies the maximum PL intensity at 400 and 800 nm. The Silica-Titania NPs configuration shows the maximum PL intensity at 800 nm in comparison to the Titania-Silica NPs configuration. High temperatures are required to reach the maximum amplitude, up to 800°C. However, if we work with the Titania-Silica NPs configuration is possible to control the maximum PL emission at 400 nm or 800 nm, with the advantage of applying lower temperatures that do not modify drastically the NPs morphology as high temperature may do, as the phase contrast shows in Figure 4. It is an important result that allows interest applications in optoelectronics devices as solar cells.

Figure 2a) shows the structure of a standard c-Si solar cell, where the band gap (Eg) is 1.12 eV. There are several processes to enhance the efficiency of a solar cell, one of these is the change of wavelength absorption given by DC materials. Also, there was observed in Figure 6a) that Titania-Silica NPs configuration performance the maximum PL emission at lower temperatures (400 and 500 °C) in the range from 3.1 eV to 3.35 eV, after to be illuminated with a wavelength of 3.54 eV. From these results is evident that silica NPs contribute more to the absorption than titania NPs in this emission region (3.1 eV), because, as has been mentioned, this emission corresponds to silica material. There is a minimal PL emission contribution of titania NPs from 1.55eV at same low temperatures. These parameters promise to be optimal to be applied in our standard solar cells. Therefore, these DC materials ensure that larger light absorption increases the current density, generating more electron-holes, and minimizing loses by heat.

The Current density (J) vs voltage (V) of the c-Si solar cells were measured before and after the NPs deposition with thermal treatment. These results are shown in Table I, the values shown are the annealing temperature at the time of 10, 20, and 30 min, current density in the short circuit density (J_{sc}), the open circuit voltage (V_{oc}), fill factor (FF), and efficiency $EFF(\eta)$.

The results showed that solar cells with Titania-Silica NPs configuration enhanced their performance characteristic. The samples annealed at 400°C for 10 and 20 min enhanced their J_{sc} in 10.28 % and 6.31%, η in 4.29 % and 1.14%, respectively, in comparison to a raw solar cell. Similarly, solar cells with the same NPs configuration at 500°C for 30 min enhance their J_{sc} in 8.57% and η in 1.14% in comparison to a bare device.

TABLE I. PERFORMANCE CHARACTERISTICS OF C-SI SOLAR CELLS SUBJECTED TO ANNEALING PROCESS FOR DIFFERENT TIMES.

Sample	Time	V_{oc}	J_{sc}	FF	$EFF(\eta)$
	min	V	mA/cm^2	%	%
Without TiO_2+SiO_2 NPs	0	0.54	32.1	0.46	8.05
With TiO_2+SiO_2 NPs at 400°C	10	0.54	35.4	0.64	12.34
Without TiO_2+SiO_2 NPs	0	0.52	30.1	0.70	11.02
With TiO_2+SiO_2 NPs at 400°C	20	0.54	32.0	0.70	12.16
Without TiO_2+SiO_2 NPs	0	0.54	33.4	0.69	12.04
With TiO_2+SiO_2 NPs at 400°C	30	0.54	32.9	0.60	10.77
Without TiO_2+SiO_2 NPs	0	0.54	34.8	0.67	12.78
With TiO_2+SiO_2 NPs at 500°C	10	0.54	33.0	0.72	13.0
Without TiO_2+SiO_2 NPs	0	0.52	34.0	0.70	12.47
With TiO_2+SiO_2 NPs at 500°C	20	0.54	33.1	0.72	13.06
Without TiO_2+SiO_2 NPs	0	0.54	31.5	0.65	11.09
With TiO_2+SiO_2 NPs at 500°C	30	0.54	34.2	0.66	12.23
Without TiO_2+SiO_2 NPs	0	0.48	27.7	0.63	8.49
Without TiO_2+SiO_2 NPs at 400°C	10	0.48	26.4	0.67	8.53
Without TiO_2+SiO_2 NPs	0	0.50	29.6	0.56	8.36
Without TiO_2+SiO_2 NPs at 500°C	30	0.48	26.7	0.50	6.46

Figure 7 shows the Current density vs voltage curves of the solar cells. The black line corresponds to a solar cell before the annealing treatment and without NPs configuration. The red line corresponds to a solar cell with thermal treatment and Titania-Silica NPs configuration. Figure 7a) shows the maximum increment of J_{sc} after the thermal treatment at 400°C for 10 min. Figure 7b) shows the J_{sc} increment at 400°C for 20 min and Figure 7c) shows the second maximum J_{sc} at 500°C for 30 min.

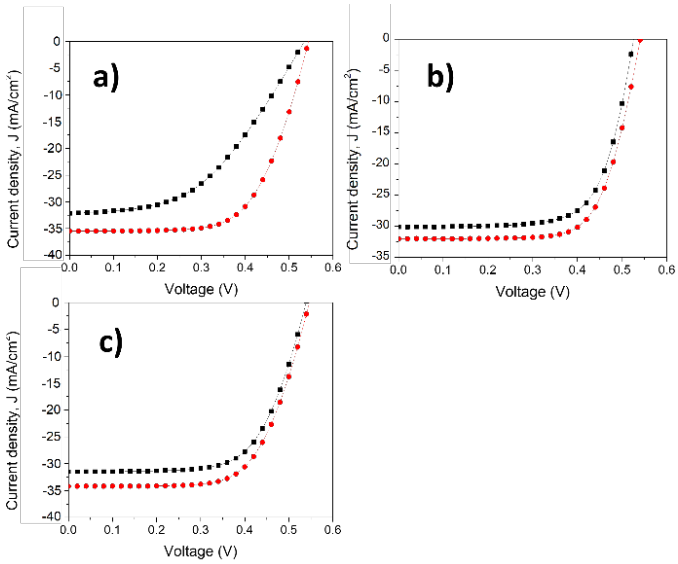

Figure 7. Current density vs Voltage curves of solar cells: before annealing process/without NPs configuration (black line) and with Titania-Silica NPs configuration/thermal treatment (red line). Thermal treatment at 400°C: a) 10 min, b) 20 min and at 500°C: c) 30 min.

Figure 8 shows the current density vs Voltage curve of solar cells without NPs before (black line) and after (red line) thermal treatment. The intention is to show that the J_{sc} is increased by the NPs deposition on top of solar cells. Therefore, the standard solar cells were subjected to 400 and 500°C for 10 and 30 min, respectively, without the NPs configuration. There is observed that the thermal process by itself does not enhance the J_{sc}.

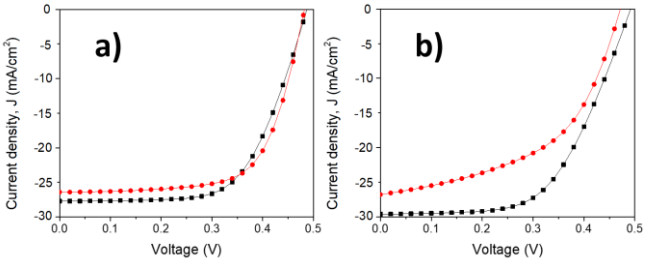

Figure 8. Current density vs Voltage curves of solar cells without NPs configuration before annealing process (black line) and after thermal treatment (red line) a) at 400°C° for 10 min and b) at 500°C for 30 min

Finally, we found that 43% of the solar cells increased their current density by 8% in average when the NPs are employed and annealed at lower temperatures. The experimental results verify that the Titania-Silica NPs configuration over the standard solar cells enhance the light absorption. For the rest of the samples, the current density was lower when the NPs were employed. Then more studies are needed to clarify this effect.

CONCLUSIONS

The characteristic PL emission of Titania-Silica and Silica-Titania NPs configurations was enhanced by thermal treatments. Our results showed that the order in which layers were deposited modified the PL emissions. We observed that the Silica-Titania bilayer NPs configuration had a larger emission than the Titania-Silica NPs configuration after the thermal process. For the Silica-Titania NPs configuration, the maximum PL emission was shifted from 400 nm to 800 nm as the temperature was increased. The Titania-Silica NPs configuration showed a shifting of the maximum PL emission from 400 nm to 800 nm as the temperature was increased and the annealing process at 400°C and 500°C for 10, 20, and 30 min produced the optimal PL emission of NPs. We found that 43 % of the solar cells increased their current density by 8 % in average when the NPs were used. For the rest of the samples, there is not an enhances in their performance characteristics. It is necessary to perform more research on the PL emission and annealing temperature on solar cells with Titania-Silica NPs configuration with potential applications in different microelectronics devices.

ACKNOWLEDGMENT

This work has been supported by the microelectronics laboratory at the National Institute of Astrophysics, Optics, and Electronics (INAOE). Carina Gutiérrez acknowledges the National Council of Science and Technology (CONACYT) of México for financial support with the scholarship number of 487557.

REFERENCES

[1] J. Sun, B. Bhushan, and J. Tong, "Structural coloration in nature," *RSC Advances*. 2013. doi: 10.1039/c3ra41096j.

[2] S. Das *et al.*, “A leaf-inspired photon management scheme using optically tuned bilayer nanoparticles for ultra-thin and highly efficient photovoltaic devices,” *Nano Energy*, 2019, doi: 10.1016/j.nanoen.2018.12.072.

[3] A. V. Ruban, “Plants in light,” *Commun Integr Biol*, vol. 2, no. 1, pp. 50–55, 2009, doi: 10.4161/cib.2.1.7504.

[4] A. V. Ruban, “Evolution under the sun: Optimizing light harvesting in photosynthesis,” *J Exp Bot*, vol. 66, no. 1, pp. 7–23, 2015, doi: 10.1093/jxb/eru400.

[5] M. B. de la Mora, O. Amelines-Sarria, B. M. Monroy, C. D. Hernández-Pérez, and J. E. Lugo, “Materials for downconversion in solar cells: Perspectives and challenges,” *Solar Energy Materials and Solar Cells*, vol. 165, no. March, pp. 59–71, 2017, doi: 10.1016/j.solmat.2017.02.016.

[6] B. S. Richards, “Novel Uses of Titanium Dioxide for Silicon Solar Cells,” 2002.

[7] A. M. Alsaad, A. A. Ahmad, A. Raouf, A. Dairy, A. S. Al-anbar, and Q. M. Al-bataineh, “Results in Physics Spectroscopic characterization of optical and thermal properties of (PMMA-PVA) hybrid thin films doped with SiO 2 nanoparticles,” *Results Phys*, vol. 19, no. October, p. 103463, 2020, doi: 10.1016/j.rinp.2020.103463.

[8] C. Gutierrez, M. Moreno, P. Rodriguez, L. Tecuapetla, A. Hernandez, and A. Itzmoyotl, “Photoluminescence emission under thermal annealing of Silica and Titania nanospheres arrays,” *2020 17th International Conference on Electrical Engineering, Computing Science and Automatic Control, CCE 2020*, 2020, doi: 10.1109/CCE50788.2020.9299206.

[9] C. Gutierrez, M. Moreno, P. Rodriguez, L. Tecuapetla, and A. Itzmoyotl, “Study of photoluminescent properties and light reflectance of silica and titania nanospheres in bilayer arrays,” no. March, p. 57, 2021, doi: 10.1117/12.2576741.

[10] R. L.-E. J. Alarcón-Salazar, A. M.-S. E. Quiroga-González, I. E. Z.-H. J. Pedraza-Chávez, and M. Aceves-Mijares, “Silicon-Rich Oxide Obtained by Low-Pressure Chemical Vapor Deposition to Develop Silicon Light Sources,” no. Cvd, Accessed: Sep. 12, 2022. [Online]. Available: http://dx.doi.org/10.5772/63012

[11] J. Barreto and C. Dom, “Optical characterization of silicon rich oxide films,” vol. 142, pp. 12–18, 2008, doi: 10.1016/j.sna.2007.03.008.

[12] E. Tu, “Investigation of Photoluminescence Mechanisms from Regime by Deconvolution of Photoluminescence Spectra,” 2016, doi: 10.1166/jnn.2016.10863.

[13] I. C. MirjanPhotoluminescence of Anatase and Rutile TiO 2 Particles †a, M. D. Dramic, D. J. Jovanovic, S. P. Ahrenkiel, and J. M. Nedeljkovic, “Photoluminescence of Anatase and Rutile TiO 2 Particles †,” pp. 25366–25370, 2006, doi: 10.1021/jp064454f.

[14] P. Account, “Atomic Defects in Titanium Dioxide,” pp. 923–934, 2014, doi: 10.1002/tcr.201402038.

[15] J. C. Hulteen and R. P. Van Duyne, “Nanosphere lithography: A materials general fabrication process for periodic particle array surfaces,” *Journal of Vacuum Science & Technology A: Vacuum, Surfaces, and Films*, vol. 13, no. 3, pp. 1553–1558, 2002, doi: 10.1116/1.579726.

[16] T. R. Jensen, M. D. Malinsky, C. L. Haynes, and R. P. Van Duyne, “Nanosphere Lithography: Tunable Localized Surface Plasmon Resonance Spectra of Silver Nanoparticles,” *J Phys Chem B*, vol. 104, no. 45, pp. 10549–10556, 2002, doi: 10.1021/jp002435e.

[17] O. Secundino-Sanchez, J. Diaz-Reyes, J.F. Sanchez-Ramırez, and J.L. Jimenez-Perez, “Structural and optical characterization of the crystalline phase transformation of electrospinning TiO 2 nanofibres by high temperatures annealing,” vol. 65, no. October, pp. 459–467, 2019.